Asymptotic normalization coefficient for the study of the mirror nuclei ^{7}Li and ^{7}Be

J. A. Pérez-Velasco[1], *J. C.* Morales-Rivera[1*], and *E.* Martinez-Quiroz[2]

[1]Facultad de Ciencias, Universidad Autónoma del Estado de México, Instituto Literario 100, Código Postal 50000, Toluca, México.
[2]Departamento de Aceleradores y Estudio de Materiales, Instituto Nacional de Investigaciones Nucleares, Apartado Postal 18-1027, 11801, México, D.F., México.

Abstract. We present a theoretical study of the nuclear structure of the mirror nuclei ^{7}Li and ^{7}Be by using the asymptotic normalization coefficient (ANC) method through the transfer reactions ^{6}Li(d,p)^{7}Li and ^{6}Li(^{3}He,d)^{7}Be. For these reactions, the elastic scattering and the transfer angular distributions were calculated considering cluster structures for the residual nucleus and the transfer particle. With the use of the Fresco code, we found the optical model parameters which reproduce the experimental data for the elastic and the transfer angular distributions and we got the ANC for the single particle model and the spectroscopic factor on the ground and the first excited states of each nuclei. This methodology allows to calculate the nuclear ANC which describes the peripheral behavior of both nuclei on their bound states.

1 Introduction

A previous work studying the fusion between ^{7}Li and ^{51}V has shown unexpected results by detecting an increase in the fusion cross section for the residual nucleus ^{52}Cr in comparison with the fusion-evaporation calculations reported. In that work, the authors propose that the overproduction of the ^{52}Cr nucleus could be explained if we consider that when ^{7}Li projectile approaches the target, ^{7}Li can be excited and the binding energy of the unpaired nucleon decreases, and the possibility that ^{7}Li radius increases in an excited state facilitating the transfer process of a proton from ^{7}Li to ^{51}V [1]. To prove this hypothesis, it is necessary to study the asymptotic behavior of ^{7}Li and its mirror nucleus ^{7}Be because both nuclei have an unpaired nucleon in the $1p_{3/2}$ shell (according to the nuclear shell model), then it is expected a similar behavior. For example, refs. [2, 3] have reported that the root mean square (RMS) for ^{13}C, in the first excited state, is almost 50% bigger than in the ground state.

The ANC for a bound state $B \rightarrow A + n$ determines the probability that the $A + n$ configuration in nucleus B can exist at greater distances than the radius of the nuclear interaction. ANCs determine the cross sections of peripheral nuclear reactions, in particular, reactions between charged particles at low energies. The most important type of such reactions is represented by astrophysical nuclear reactions [4, 5]. Besides, the information that the ANC provides about the distribution of matter in the nucleus allows the calculation of the root mean square [6]. The RMS of both nuclei are going to be calculated and compared with the classic size nuclear in a future work.

*e-mail: jmoralesriv@uaemex.mx

To achieve this, we used the Fresco code, created in 1983 by Ian Thompson to perform coupled reaction channel calculations for the three-body interactions [7]. Using this code, it was possible to calculate the angular distributions that best fit the experimental data for the transfer reactions and the elastic scattering, simultaneously. The bound state wave function $\Psi_{An}(r)$ can be approximated by means of the equation (1)

$$\Psi_{An}(r) \rightarrow C_{An}\frac{W}{r} \tag{1}$$

Where C_{An} is the nuclear ANC of the bound state $B \rightarrow A + n$ and W is the Whittaker function.

2 Theoretical Analysis

For this analysis the experimental data were taken from Lüdecke and Schiffer [8, 9]. Schiffer studied the transfer angular distribution for the reaction ^{6}Li(d,p)^{7}Li at 12 MeV while Lüdecke studied the elastic scattering at 11.8 MeV and the transfer and elastic scattering angular distributions for the reaction ^{6}Li(^{3}He,d)^{7}Be at 10 MeV.

The sets of the optical model potential parameters used by these authors are shown in Table 1. However, the usage of these parameters is not convenient because they do not fit to the elastic scattering and the transfer angular distributions simultaneously: a good fitting in the stripping data results in a bad fitting for the elastic scattering data [8].

Five sets are shown in Table 1; sets I and II have a good fit in the elastic scattering of ^{3}He on ^{6}Li while Sets I' and II' work well in the scattering of deuterons on ^{7}Li but they do not fit in the transfer angular distribution, while Set III was used to study only the transfer angular distribution.

Table 1. Optical Model Parameters reported by the authors, *Sets I, II, I', II'* were taken from reference [8] while *Set III* is from [9].

	Depth (MeV)	r_V (fm)	a_V (fm)
Set I	V=140.00	1.30	0.29
	W= 7.50	2.31	0.57
Set II	V= 140.00	2.00	0.58
	W= 30.00	2.00	0.74
	S.O.=6.00	1.20	0.70
Set III	V= 118.00	0.88	0.90
	W= 5.80	1.57	0.77
	S.O.=5.80	0.88	0.90
Set I'	V= 118.00	0.87	1.00
	W= 6.90	1.71	0.89
	S.O.=7.50	1.71	0.89
Set II'	V= 78.00	1.04	0.95
	W= 30.00	0.85	0.85
	S.O.=12.50	0.85	0.85

To get the parameters that fit the transfer and the elastic scattering angular distributions simultaneously, the sets from Table 1 were modified to better fit to the experimental data. The new parameters obtained are shown in Table 2 and Table 3.

2.1 Angular Momentum Conservation

During nuclear reactions, there must be a conservation of orbital and spin angular momentum. There must also be a parity conservation, because of that, it was necessary to calculate the allowed values of momentum for each nucleus according to the standard angular-momentum coupling scheme (equations 2-5) [10].

$$\boldsymbol{I_a} = \boldsymbol{j_1} + \boldsymbol{I_b} \qquad \boldsymbol{I_A} = \boldsymbol{j_2} + \boldsymbol{I_B} \tag{2}$$

$$\boldsymbol{j_1} = \boldsymbol{l_1} + \boldsymbol{s_p} \qquad \boldsymbol{j_2} = \boldsymbol{l_2} + \boldsymbol{s_p} \tag{3}$$

$$\boldsymbol{L} = \boldsymbol{j_1} + \boldsymbol{j_2} = \boldsymbol{l_1} + \boldsymbol{l_2} \tag{4}$$

$$P_a = (-1)^l P_b \tag{5}$$

Where l_1 and l_2 are the orbital angular momenta while j_1 and j_2 are the transferred angular momenta of relative motion of the transfer particle. Equation (4) is the total transferred angular momentum, and finally equation (5) is for the parity conservation. These equations were used to find the allowed values of momentum for the core and the transfer particle for every studied reaction. We calculated then the contribution of each value to the transfer.

For the reaction ^{6}Li(^{3}He,d)^{7}Be, considering that the transfer particle is a proton with $1/2^+$ angular momentum, the allowed angular moment values for the proton interaction are $J^\pi = \frac{1}{2}^+$ and $J^\pi = \frac{3}{2}^+$ on the ground state and are the same values on the first excited state. For the reaction ^{6}Li(d,p)^{7}Li, the transfer particle is a neutron with $1/2^+$ angular momentum, the allowed angular moment values for this configuration are also $J^\pi = \frac{1}{2}^+$ and $J^\pi = \frac{3}{2}^+$ on both states.

Table 2. Optical Model Parameters for ^{6}Li(^{3}He,d)^{7}Be. Potential 1 and 1' represent the real and imaginary Woods-Saxon interaction, respectively. Potential 2 refers to the Woods-Saxon surface potential and 3 to the Spin-Orbit interaction.

	Potential	V (MeV)	r_V (fm)	a_V (fm)
^{3}He+^{6}Li	1	110.00	1.00	0.68
	1'	40.00	1.00	0.20
	3	6.00	1.36	0.18
d+^{7}Be	1	44.00	1.15	0.81
	2	2.15	1.34	0.87
	3	6.00	1.15	0.81
d+p	1	52.00	1.25	0.50
	2	4.59	1.20	0.51
^{6}Li+p	1	85.00	1.05	0.60
	2	10.15	1.33	0.50
	3	12.15	1.02	0.20

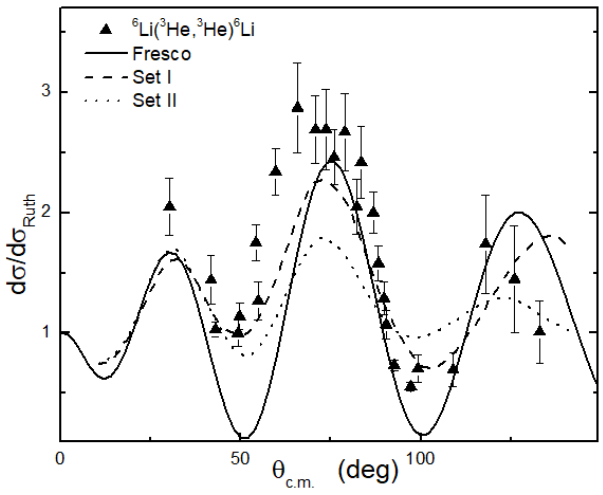

Figure 1. Elastic scattering angular distribution for ^{3}He+^{6}Li at 10 MeV. The solid line shows the obtained results using parameters from Table 2 while dashed lines use the parameters from *Set I* and *Set II*, listed in Table 1.

2.2 The ^{6}Li(^{3}He,d)^{7}Be reaction

In the study of both reactions the four potentials were considered; the entrance channel, the exit channel and the bond potentials for the projectile and the residual nuclei. Parameters from Table 2 were used in Fresco, and we got the angular distribution for elastic scattering (Figure 1) and transfer (Figure 2).

Figure 1 shows the elastic scattering angular distribution for ^{3}He on ^{6}Li at 10 MeV. It is possible to see that parameters from Table 2 provides a good fit from 73 to 115° and the curve calculated with Fresco reproduces the shape of the experimental data curve. The dashed and dotted lines are the curves calculated with the parameters from Table 1.

Figure 2 shows a good fit for the transfer experimental data on the ground and first excited state (0.431 MeV, $1/2^-$), both curves were normalized to the experimental

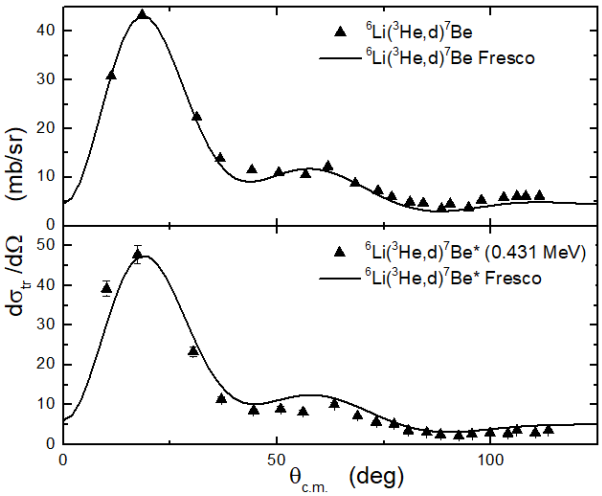

Figure 2. Transfer angular distribution for ^{6}Li(^{3}He,d)^{7}Be at 10 MeV on the ground state and the first excited state with an energy 0.431 MeV.

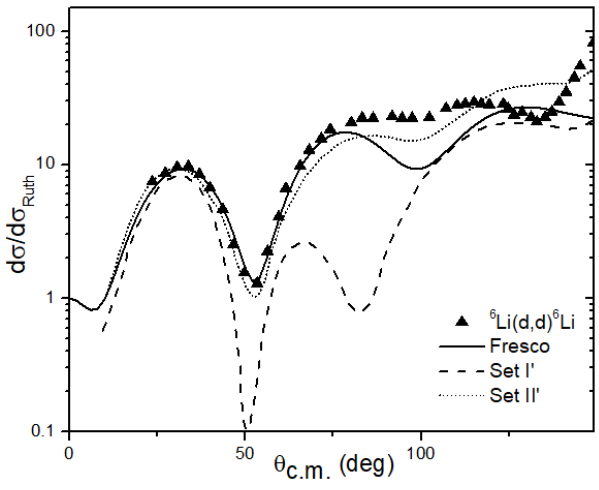

Figure 3. Elastic scattering angular distribution for d+^{6}Li at 11.8 MeV. The solid line shows the results using parameters from Table 3 while dashed and dotted lines show the results using *Set I´* and *Set II´*.

Table 3. Optical Model Parameters for ^{6}Li(d,p)^{7}Li. Potential 1 and 1' represents the real and imaginary Woods-Saxon interaction, respectively. Potential 2 is for the Woods-Saxon surface potential and 3 represents the Spin-Orbit interaction.

	Potential	V (MeV)	r_V (fm)	a_V (fm)
d+^{6}Li	1	120.00	0.83	0.79
	1'	40.24	1.50	0.20
	3	5.80	0.83	0.79
p+^{7}Li	1	44.00	1.15	0.81
	2	1.40	1.34	0.87
	3	6.00	1.15	0.81
n+p	1	52.00	1.25	0.50
	2	4.59	1.20	0.51
^{6}Li+n	1	85.00	1.05	0.60
	3	12.15	1.02	0.20

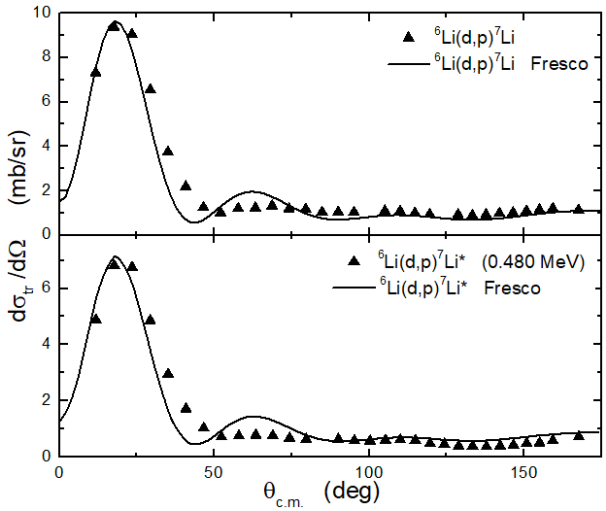

Figure 4. Transfer angular distribution for ^{6}Li(d,p)^{7}Li at 12 MeV on the ground state and the first excited state with an energy 0.480 MeV.

cross sections in the region of the main maximum of the angular distribution. This normalization allows us to determine the spectroscopic factor S for each J^π calculated.

2.3 The ^{6}Li(d,p)^{7}Li reaction

The used optical model parameters for this reaction are shown in Table 3, those were used in the input, and Fresco calculated the angular distribution for the elastic scattering (Figure 3) and for the transfer (Figure 4).

In Figure 3 it is possible to see that the curve created with the parameters from Table 3 fits very well from 0 to 75° and still close to the experimental data curve at higher angles. The dashed and dotted lines correspond to Sets I' and II'. Sets I' and II' have a good fit in the elastic scattering, but they does not work for the transfer angular distribution.

Figure 4 shows the fitting of the transfer angular distribution calculated with Fresco to experimental data for Lithium on the ground and first excited state (0.480 MeV); as before both curves were normalized to the first maximum and then the spectroscopic factor was calculated.

Every J^π has an individual contribution to the total transfer section. After calculating this contribution and with the normalization to the first maximum of the transfer cross section we got the individual spectroscopic factor in the single particle model ($S^{(sp)}$) for each J^π (see Tables 4 and 5).

3 Extraction of ANCs

If we consider a cluster structure $B = (A + n)$, where A represents the core and n the valence particle. The ANCs determine the asymptotic behavior of the wave functions

Table 4. Asymptotic Normalization Coefficients for ^{7}Be

Ground state				
J^{π}	b_{An} $(fm^{-1/2})$	$S^{(sp)}$	C_{An} $(fm^{-1/2})$	C_{An} average $(fm^{-1/2})$
$\frac{1}{2}^{+}$	2.39	0.72±0.05	2.03±0.07	1.93±0.09
$\frac{3}{2}^{+}$	2.69	0.48±0.03	1.87±0.06	
First excited state				
J^{π}	b_{An} $(fm^{-1/2})$	$S^{(sp)}$	C_{An} $(fm^{-1/2})$	C_{An} average $(fm^{-1/2})$
$\frac{1}{2}^{+}$	2.23	1.48±0.10	2.71±0.09	2.62±0.12
$\frac{3}{2}^{+}$	2.50	1.02±0.07	2.53±0.09	

Table 5. Asymptotic Normalization Coefficients for ^{7}Li

Ground state				
J^{π}	b_{An} $(fm^{-1/2})$	$S^{(sp)}$	C_{An} $(fm^{-1/2})$	C_{An} average $(fm^{-1/2})$
$\frac{1}{2}^{+}$	5.67	0.39±0.03	3.56±0.13	3.52±0.18
$\frac{3}{2}^{+}$	5.33	0.42±0.03	3.48±0.12	
First excited state				
J^{π}	b_{An} $(fm^{-1/2})$	$S^{(sp)}$	C_{An} $(fm^{-1/2})$	C_{An} average $(fm^{-1/2})$
$\frac{1}{2}^{+}$	5.35	0.53±0.04	3.89±0.14	3.86±0.19
$\frac{3}{2}^{+}$	5.00	0.59±0.04	3.83±0.13	

of the B nuclei and thereby provide the probability that the binary channel $A + n$ can exist [11].

Fresco calculates and gives in the output the ANC for the simple particle model for each allowed value of angular momentum and we have already calculated the S factor for each J^{π}.

Then, the single-particle spectroscopic factor $S^{(sp)}$ relates the single-particle ANC b with the nuclear ANC C using the equation (6). The results obtained are shown in Tables 4 and 5.

$$C_{An} = b_{An}\sqrt{S^{(sp)}} \tag{6}$$

4 Conclusions

We calculated the angular distributions for the elastic scattering and transfer for the reactions ^{6}Li(^{3}He,d)^{7}Be and ^{6}Li(d,p)^{7}Li using a set of optical model parameters which simultaneously fits better both distributions. We used this methodology for the ground and the first excited states of ^{7}Li and ^{7}Be.

With the obtained optical model parameters and using Fresco we extracted the ANC for the simple particle model, while the normalization of the transfer distribution gave the spectroscopic factor for every allowed angular momentum value of each bound state. After averaging this information and calculating the uncertainty we could determine the nuclear asymptotic normalization coefficient for the ground and the first excited states of the ^{7}Li and ^{7}Be nuclei.

These Asymptotic Normalization Coefficients allow us to describe the peripheral behavior because with them we can approximate the bound state wave function, which is the first step for a more complete study of the nuclear structure and the calculation of the root mean square of both mirror nuclei.

References

[1] J. C. Morales Rivera. *Estudio teórico y experimental del sistema $^{9}Be+$ ^{51}V y sistemas similares*, Ph.D. Thesis, Universidad Autónoma del Estado de México (2019).
[2] Z. H. Liu *et al.* Phys. Rev. C **64**, 034312 (2001).
[3] T. L. Belyaeva, *et al.*, EPJ Web of Conf. **66**, 03009 (2014).
[4] K. I. Tursunmakhatov, and E. Sh Ikromkhonov. Int. J. of Mod. Phys. E **32**, 2350035 (2023).
[5] L. D. Blokhintsev, Phys. of Part. and Nucl. **53**, 482 (2022).
[6] E. T. Li, *et al*., Chinese Phys. C, **40**, 114104 (2016).
[7] I. J. Thompson, Comp. Phys. Rep. **7**, 167 (1988).
[8] H. Lüdecke *et al*., Nucl. Phys. A **109**, 676 (1968).
[9] J. P. Schiffer *et al.*, Phys. Rev. **164**, 1274 (1967).
[10] T. L. Belyaeva *et al.*, Phys. Rev. C **80**, 064617 (2009).
[11] R. Yarmukhamedov *et al.*, Uzb. J. Phys. **12**, 233 (2010).